Imaging in Complex Media

Jacopo Bertolotti[1] and Ori Katz[2]

[1]Physics and Astronomy Department, University of Exeter, Stocker Road, Exeter EX4 4QL, UK
[2]Department of Applied Physics, Hebrew University of Jerusalem, 9190401 Jerusalem, Israel

Abstract

Imaging can take many forms — from optical microscopes and telescopes, through ultrasonography, to x-ray tomography. However, no matter the imaging modality, the presence of a complex heterogenous structure between the imaging system and the scene of interest limits the quality of the images that can be conventionally obtained. In this Review article, we give an overview of the recently introduced strategies to overcome the detrimental effects of scattering in optical imaging. In particular, we focus on approaches that either physically correct scattering using computer–controlled devices or employ computational inversion based on intrinsic correlations of light scattering. Despite focusing on optical techniques, this Review article emphasizes the fundamental equivalence of the effects of scattering in different fields of imaging, using the scattering-matrix formalism as a bridge that allows techniques developed in one field to be translated to another.

1 Introduction

Imaging is an umbrella term used for a large variety of techniques aimed at forming a representation of an object's spatial distribution. The simplest and most common forms of optical imaging use a lens to reproduce the intensity of the light scattered from an object on an image plane where it can be measured by a multipixel detector array — a camera. This works because in free-space propagation, a lens can create a reliable one-to-one mapping between each point on the imaged plane and each point on the detector. However, if light is scattered during its propagation this relationship is broken, the light from each point on the object is spread to many camera pixels, and the quality of the image is degraded. How much the quality of the image degrades depends upon how and how much of the light is scattered. This is dictated by the medium properties, and can be characterized by the medium's transport mean free path, ℓ_t [1]. For a collimated light beam, the fraction of light still unscattered after traversing a scattering medium of thickness L, will be given by the Lambert-Beer law:

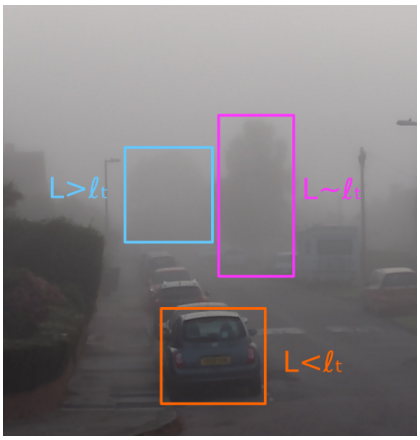

Figure 1: Imaging through fog provides an example for optical imaging through complex media. Fog is composed of small water droplet that scatter visible light, preventing the formation of a clear image. Imaging through a layer of fog thinner than a characteristic distance, known as the transport mean free path ℓ_t, will result in a slightly degraded image, but if the thickness L of the fog layer is much bigger than ℓ_t, no image can be formed at all.

e^{-L/ℓ_t} [2].
As shown in Fig.1, at a distance $L < \ell_t$ only a small fraction of light has been scattered, and the reduction in imaging quality is minimal. On the other hand, at a distance $L \sim \ell_t$, a significant fraction of the light has been scattered, resulting in a blurry background, obscuring the object features. Finally, for $L >> \ell_t$ essentially all of the light has been scattered and the conventional image degrades to the point where no sharp object features can be seen(fig.1) [3].
Whether a sample is scattering or not also depends on the type of wave used for imaging. For example, soft tissues scatter visible light, but not x-rays or ultrasound. Similarly, concrete walls scattering (and absorb) light and sound, but affect radio-frequency waves much less. As a consequence, two direct approaches to avoid scattering are to either modify the medium or the imaging modality. Examples include tissue clearing by chemical means [4] and the use of x-rays to image inside the body [5]. Despite the existence of techniques that turn scattering into a non-problem, there are situations where none of these options are viable. Such is the case where the medium cannot be altered, when ionizing radiation, such as x-rays, is undesired, or when the contrast or resolution provided by the non-scattered waves is insufficient. For example, the non-microscopic resolution of ultrasound imaging cannot resolve cellular structures [6]. In this Review article we describe the main techniques that have been developed to tackle scattering, with a focus on the recent developments in optical imaging, but with the goal of highlighting the fundamental similarities between different fields and approaches.

2 Imaging by filtering out scattered light

In many instances of imaging in volumetric scattering media — particularly at depths below ℓ_t — a small fraction of light remains unscattered. One option to improve imaging is therefore to use only this small portion of unscattered — or 'ballistic' — light to form the image. This approach has the advantage that, because the light used for imaging was never disturbed, one can directly reconstruct very sharp images.

There are different approaches to separate the scattered and unscattered light. One option is to time-gate the light by sending short pulses to illuminate the scene and then measure only the light arriving at a given time. As the diffused background travels through many different paths, it is temporally broad, and a short time-gate preferentially selects the light that bounced back from the object but was otherwise unscattered. This approach has the additional advantage of providing a measurement of the distance, allowing a 3D reconstruction, and is thus commonly used in light detection and ranging (LiDAR) [7]. For time-gating to work, the time gate has to be much shorter than the typical temporal spread of the signal. Time gating can be achieved using fast detectors, or by low-coherence interferometry using a short temporal-coherence source, which is the basis for optical coherence tomography (OCT) [8].

A different approach to preferentially measure unscattered light is spatial gating, which aims at preferentially measuring the light that originated from a specific illuminated point in the medium. The idea is that when focused illumination and an imaging system are used, the scattered light would be spread over a large area in the detector plane, whereas the unscattered light would be concentrated around the imaged illumination point. This is the principle behind confocal microscopy [9]. Another effective approach for spatial gating is to use nonlinear signal generation mechanisms, such as harmonic frequency generation or multiphoton fluorescence excitation [10]. Multiphoton microscopy exploits the fact that nonlinear signals are preferably generated at the focus, where the instantaneous intensity is the highest [11], and has recently achieved imaging at depths approaching ℓ_t [12].

The main limitation of gating-based approaches is that there is always a small fraction of scattered light that incidentally underwent a path of exactly the same length and direction as the unscattered ballistic light and the intensity of the unscattered light decays exponentially with depth. Therefore, at sufficiently large imaging depths, the detected intensity of the unwanted scattered waves, which decay linearly with depth, will be higher than that of the desired unscattered waves [13]. Although the exact values depend on the details of the medium and specific technique, such 'filtering' approaches tend to work up to thicknesses comparable to ℓ_t, and degrade quickly beyond that. To reach larger depths one must therefore use scattered light for imaging, rather than discard it.

3 Imaging with scattered light

3.1 The scattering-matrix formalism

When imaging at depths beyond ℓ_t, one has no choice but to form the image from the (multiply) scattered light [14]. As in nearly all practical optical imaging situations the light intensities involved are too low to induce significant nonlinear interactions outside the focus, light propagation in complex media can be considered linear. As a consequence, the scattered optical field measured after propagation through a complex medium is a linear sum of the medium's response to the field at each point in the input plane (Fig.2a).

Formally, the propagation through a complex medium is described by a set of Green functions, $G(r_{in}, t_{in}, r_{out}, t_{out})$, connecting the input field at each position coordinate r_{in} and time t_{in} (for example, the field at the target object plane, $E^{in}(r_{in}, t_{in})$) with the output field at each output position coordinate, r_{out}, at a time t_{out} (for example, the field at the camera plane, $E^{out}(r_{out}, t_{out})$). If the scattering medium response is time-invariant, the Green function depends only on $t = t_{out} - t_{in}$, and one can perform a Fourier transform with respect of time to obtain the complex-valued input-output relation at each angular frequency ω: $G_\omega(r_{in}, r_{out})$. For simplicity, we will consider the case of monochromatic excitation, where the input-output relations are given by the single-frequency response: $E^{out}(r_{out}) = \iiint G_\omega(r_{in}, r_{out}) E^{in}(r_{in}) d^3 r_{in}$.

In the spatial domain, the field can be decomposed into discrete spatial channels: $E_n(r)$ (with $n = 1 \dots N$). Thus, the medium's Green functions can be discretized in space, and written as a single complex-valued matrix, $\mathbf{S}$ (for each frequency ω). This 'scattering matrix', fully describes the medium response in both transmission and reflection (for a more detailed discussion, see [15]). Each of its elements, $\mathbf{S}_{m,n}$, describes the response at the m^{th} output mode for excitation of the n^{th} input mode (Fig.2a-b). In the scattering-matrix formalism, the output field is given by the matrix multiplication between the scattering matrix and the input field: $E^{out} = \mathbf{S} E^{in}$, that is, $E^{out}_m = s_{m,n} E^{in}_n$.

Each scattering matrix column $n = 1 \dots N$ thus gives the Green function (impulse response) of the medium to excitation by the input mode n (Fig.2b). One has the freedom to choose which basis to use for the field decomposition. Although the real-space and k-space bases are two very natural and common choices in optics, other bases, such as transmission eigenchannels [16, 17], principal modes [18] or singular vectors [13], sometimes provide valuable insights on the physics of the system. It is often useful to separate the scattering matrix into 'transmission' (T) and 'reflection' (R) matrices, describing the medium response in transmission and reflection, respectively.

As the scattering matrix formalism describes any linear transformation, it can also describe the wave propagation — for any kind of wave, not only light — from a target object to the image plane of any linear imaging system, taking into account both the complex medium and imaging optics. In optical imaging, the image formed by a single point source is known as the point spread function (PSF) [19]. The columns of the transmission matrix in the canoni-

cal basis thus represent the coherent (field amplitude) PSF of each point in the object plane. Fig.2c-k provide three representative numerical examples of transmission matrices for three common practical imaging scenarios: Firstly, the ideal case of a well-designed isoplanatic optical system imaging through a non-scattering homogeneous medium (Fig.2c-e). In this case, the imaging PSF is a high-contrast diffraction-limited spot, the transmission-matrix in the canonical basis is a nearly-diagonal matrix (that is, all points have the same PSF), and the formed image is a sharp diffraction-limited representation of the object. Secondly, atmospheric turbulence or an imperfect imaging system comes with smooth, large-scale inhomogeneities (compared to the wavelength) that produce low-order aberrations, resulting in a wider PSF with a possibly non-flat phase response (Fig.2f-h). Finally, there is imaging through multiply-scattering turbid media. Here, the field from each input point is scattered multiple times, and the interference between the different paths generate a complex speckle pattern (Fig.2i-k), with sharp bright and dark spots of diffraction-limited dimensions: $\sigma_x \approx \lambda/NA$, where λ is the wavelength, and NA is the numerical aperture [20]. While the transmission matrix of a complex medium is the result of multiple scattering, it is not a completely random matrix, but, perhaps surprisingly, possesses inherent correlations [15].

The most widely exploited type of correlations for imaging is the so called optical memory-effect for angular speckle correlations, which represents the inherent tilt invariance (or isoplanatism) of scattering through media of finite thickness [21, 22]. It can be expressed as a similarity in the structure of speckle patterns generated at the image plane by light that originates from nearby points at the object plane (see Box 1). The memory-effect correlations are, in essence, correlations between the scattering matrix columns when represented in the appropriate basis — in the plane-wave basis for a bare scattering medium or the canonical basis of a focused imaging system. Fig.2k provides an example. The correlations are clearly visible as diagonal smears, signifying the shift invariance of the scattering PSF in this imaging configuration. The angular range of the memory effect is thus the same isoplanatic angle — also known as the isoplanatic patch — used in adaptive optics [23], and ultrasound imaging [24]. Indeed, the generality of the scattering-matrix formalism is not only useful for analyzing optical imaging approaches, but allows its common use in other domains, from ultrasound [24, 25] to geophysics [26].

3.2 Diffuse optical tomography

When the goal is to only image rather large object features compared to the imaging depth, at depths considerably larger than ℓ_t, then such low-resolution imaging is possible even if the scattering matrix is not explicitly known. In such a case, the amplitude of the average spatial envelope of the scattering PSF, neglecting interference, i.e. the diffusive blurry halo, is well described by a diffusion approximation [2]. If the geometry and scattering properties of the sample and system are known, it is possible to compute the spatial distribution of the average intensity for each point of illumination [3]. In this fashion,

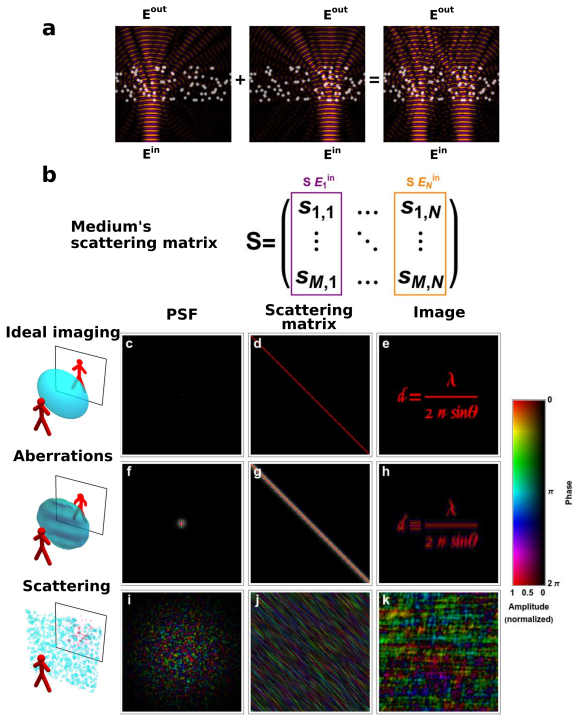

Figure 2: Scattering-matrix formalism describing linear field-propagation from an input (object plane) to an output (e.g. image plane): **(a)** Due to the linearity of the problem, even after multiple scattering, the field produced by two sources is still the sum of the fields produced by each source separately (plotted here for a monochromatic case). **(b)** At each frequency, the scattered field is given by a matrix multiplication of the complex-valued scattering-matrix, $\mathbf{S}$ with the input field: $E^{out} = \mathbf{S}E^{in}$. Each column of $\mathbf{S}$ is the response to an input, i.e. a Green function. In the canonical basis, a column of $\mathbf{S}$ is the field point spread function (PSF). **(c-k)** Numerical examples of the PSF (left), a slice of the $\mathbf{S}$ matrix (centre), and the resulting image (right) for several common imaging scenarios: **(c-e)** An ideal, free-space, imaging system. **(f-h)** Imaging through low-order aberrations, as in weak atmospheric turbulence. **(i-k)** Imaging through a strongly scattering medium, where multiple scattering dominates.

a coarse-grained intensity-only transmission matrix of the medium, which describes the forward problem, can be constructed, and retrieval of deep-lying objects can be attempted by linear inversion. This is the principle behind Diffuse Optical Tomography (DOT) [27]. As the coarse-grained forward diffusion problem effectively models scattering as blurring by a large Gaussian-like convolution kernel with a width of the order of the imaging depth, DOT can image inside strongly scattering media with a resolution of the order of the imaging depth [28].

3.3 Computational imaging using a known transmission matrix

In the scattering matrix framework, imaging in complex media can be interpreted as the reconstruction of the input field distribution, $E_{in}(x, y, z)$, from measured output fields (scattered light) distributions: $E_{out} = \mathbf{S}E_{in}$. In principle, if the scattering matrix from the object plane to the image plane $\mathbf{S}$ is known exactly, it is possible to calculate the input field using the matrix inverse S^{-1}. In practice though, experiments are often limited to measuring only the transmission ($\mathbf{T}$) or reflection ($\mathbf{R}$) part of $\mathbf{S}$. Combined with measurement noise, this makes the exact inversion impossible. Nonetheless, it is possible to estimate the input field via the pseudo-inverse operator using a variety of well-established linear inverse problem approaches, such as the Moore-Penrose pseudo-inverse and Tikhonov regularization [29]. Improved reconstruction can be obtained using compressed-sensing reconstruction algorithms when priors on the object are available [30].

However, although the transmission matrix can be directly measured if one has access to both the input (object) plane and the output plane of the scattering medium [31], as was indeed exploited in works that used a fixed random medium as a scattering lens [32, 33]), such 'invasive' access to the object plane is usually impossible in practice. Such is the case when noninvasive imaging through tissue is desired, and the imaging system cannot directly measure the single-pass transmission matrix from the object to the imaging system. A contemporary major challenge, and the focus of the remainder of this Review article, is in approaches that can estimate $\mathbf{T}$ or E_{in} from noninvasive measurements made without accessing the object plane.

Box 1: The optical memory effect
Multiple scattering turns the imaging PSF into an apparently random speckle pattern. However, even after multiple scattering, the scattered light continues to contain correlations that can be exploited for imaging. One of these correlation, which has recently found ample use in imaging, is the so-called optical memory effect. A slight tilt of the illumination angle of a scattering medium results in an identical tilt of the speckle pattern at the medium's output facet, keeping its internal structure, rather than completely randomizing it. (Fig.3a) [21, 22]. One can understand the origin of this effect by considering that illuminating a point on a facet of a diffusive sample with a pencil-like beam, results in a bright diffusive blur only around the illumination point. Thus, the transmission-matrix of the sample in the spatial position basis, $T_{r_{in},r_{out}}$, would be concentrated around the $r_{in} - r_{out}$ diagonal. The memory-effect angular correlations become visible by inspecting this transmission matrix in the Fourier ($k_{in} - k_{out}$) basis (Fig.2j)[34, 22]. As the spatial extent of the diffusive blur grows with the medium thickness, L, the angular correlation range scales as $\propto \lambda/L$.
An important consequence of the optical memory effect is that the PSFs from sources close to each other are similar, and thus the scattering from all sources within a given region (the isoplanatic patch) can be corrected with the knowledge of only a single PSF (Fig.3b), forming the basis for most adaptive optics and several wavefront-shaping techniques (see section 3.4.2), as well as ultrasonic imaging [24]. Interestingly, the angular memory effect is also present in light propagation through multi-core fibres, which opens the path to lensless diffraction-limited endoscopy (see Fig.3c, and section 3.5).
The major limitation of using the memory effect for imaging is its small field of view when imaging through thick samples. In such cases, the imaging field of view (FoV$\approx \frac{\lambda}{\pi L} d$, where $d \simeq L$ is the distance between the object and the front facet of the scattering medium) is too small for most applications. Nonetheless, the FoV can be larger when imaging an object located at a large standoff distance from a thin scattering layer (an 'eggshell' geometry) or for non-line-of-sight (NLOS) imaging 'around-corners' using light reflected from a scattering wall, where the angular memory-effect range in reflection is $\Delta\theta_{mem} \approx \lambda/(\pi\ell_t)$ [22, 35] (for alternative approaches of NLOS imaging see [36]). The FoV can also be significantly larger when imaging through biological tissues at depths smaller than ℓ_t [37] or when time-gated measurements are used [38].
Beyond angular-correlations, additional inherent correlations are present in some scenarios. For example, anisotropic scattering in soft tissues of moderate thickness (compared to ℓ_t) gives rise to speckle correlations also for transverse translations of the incident wavefront [34, 39].

3.4 Adaptive optics and wavefront shaping

3.4.1 Adaptive optics

In the case where absorption is negligible, the scattering matrix is unitary, and can thus be interpreted as a rotation in a high-dimensional space [3]. If the full

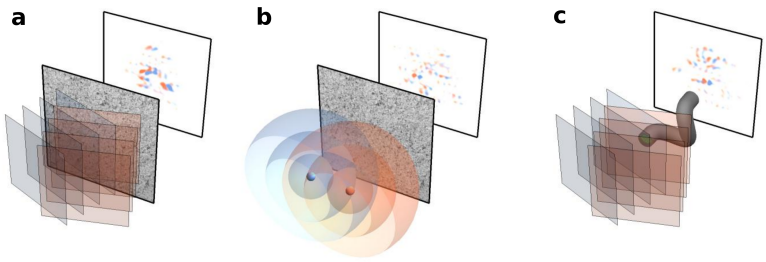

Figure 3: The angular memory effect. A correlations between the scattering-matrix columns in the k-space basis (Fig.2k). It manifests as: **(a)** plane waves that illuminate the medium at similar angles, produce similar speckle patterns, with the same angular shift as the illumination beams; **(b)** light from adjacent points is scattered into similar speckle patterns, with an angular shift between them. The same effect is also present through multicore fibres **(c)**, and in back-scattering from complex samples, such as white-painted walls..

matrix is known or can be measured, scattering can be inverted not just computationally but also physically, by applying an equal and opposite rotation using a wavefront correcting device with a sufficient number of controllable elements (degrees of freedom, or modes). Such a device can be realized by deformable mirrors (DMs) or spatial light modulators (SLMs). This is the principle for correcting low-order aberrations by adaptive optics, which was pioneered for astronomical observations [23] (Fig.2f-h). Today it is possible to near-perfectly correct atmospheric distortions in astronomical observations [23] and isoplanatic sample-induced aberrations in microscopy [40], as long as the number of controllable elements is larger than the number of scattered modes. The wavefront correction is determined by either measuring the wavefront distortions of light originating from one or several points located behind the aberrating medium — these are callled guide stars — or by varying the correction to optimize an image metric [40, 41]. The correction can be extended beyond a single isoplatic patch with the help of multiple guide stars and multiple SLMs or DMs.

3.4.2 Wavefront shaping

When the number of scattered modes, N_{modes}, increases beyond the number of controllable degrees of freedom, N_{SLM}, for example, in deep-tissue imaging, where the number of scattered modes can easily exceed 10^6, it becomes practically impossible to measure and correct all of the scattered modes. In this deep multiple-scattering regime, light forms complex speckle patterns (Fig.2i) and the scattering matrix stops being even approximately diagonal (Fig.2j). However, it is still possible to manipulate the scattered light to a useful degree and form a high contrast diffraction-limited focus on the target by enhancing the intensity of a single speckle grain through constructive interference of the

controlled modes (Fig.4b, inset). Strikingly, even though $N_{\mathrm{SLM}} \ll N_{\mathrm{modes}}$, as long as the controlled scattered modes are independent, the intensity of the wavefront-corrected focus would be approximately N_{SLM} times higher than the average intensity of the residual speckle background, which remains due to the imperfect correction [42]. Since hundreds to 10^5 modes are today routinely controlled with state-of-the-art SLMs, high-contrast focusing that can be effective for imaging can be obtained, and the imperfect correction manifests only in a lower contrast compared to perfect focusing (Fig.4b, inset). This fact forms the basis for the field of optical wavefront-shaping [43, 44]. The border between adaptive optics and wavefront shaping is not sharply defined, and a continuum exists in between these extremes, which includes relevant applications, such as the correction of low-order aberrations without undoing scattering [40].

If the scattering matrix is known, the correction wavefront for maximizing the focused intensity at a point r_m on the target is given by phase-conjugating the m^{th} row of the scattering matrix (in the canonical basis): $E_n^{SLM,in} = s_{m,n}^*$. The output field at r_m would then be: $E_m = \sum_n s_{m,n} s_{m,n}^*$, and its intensity would be maximized because the phase-conjugated input effectively forms a matched filter for the scattering. However, when the scattering matrix is not known, the focusing SLM pattern can be found by an iterative search for the input wavefront that will form a bright focus after it is scattered. In its simplest implementation, directly — and invasively — measuring the intensity at the desired focus location [45] provides the feedback for the iterative optimization. A welcome side effect is that multiple scattering usually results in large scattering angles, which can be exploited to increase the effective numerical aperture (NA) of the focused wavefront, generating a focus with dimensions smaller than the diffraction limit of the optical system in free space [32, 46]. In the near field, this scattering-lens effect can even be exploited for sub-wavelength focusing [32, 33], as first demonstrated at microwave frequencies [47].

Devising schemes that provide noninvasive feedback for diffraction-limited focusing has been of intense research in recent years. The goal is to find the focusing wavefront with the help of measurements from detectors placed outside the sample (Fig. 4a). These state-of-the-art approaches make use of a large variety of physical mechanisms and computational methods [14]. Exploiting nonlinear signal generation mechanisms, such as multiphoton excitation of fluorescence, or harmonic generation, allows diffraction-limited focusing by optimizing the total scattered nonlinear signal [48, 49, 50, 51]. In the case of linear incoherent signal generation, such as fluorescence, using the scattered light image contrast as feedback for wavefront-shaping can lead to focusing [52, 53], because when light is focused to a single point, the scattered fluorescence pattern has a maximal contrast. Similarly, the correction wavefront needed to obtain a sharp focus can be non-invasively found by directly optimizing an image sharpness metric [54]. When the signal originates from a relatively small number of fluorescent emitters, non-negative matrix factorization of a matrix containing measured scattered fluorescence patterns allows noninvasive focusing [55]. In the case of spatially-coherent signals, the spatial autocorrelation of

the scattered light pattern can be used as a feedback mechanism for focusing, exploiting the memory ffect [56].
Non-invasive focusing can also be obtained by computational decomposition of the reflection matrix, either using singular value decomposition [13, 57] or more advanced computational algorithms that aim at decomposing the scattering at the excitation and detection paths [58]. If the structure of the scattering medium can be measured or modelled, the correction wavefront can be estimated computationally [59].

The major drawback of iterative optimization or matrix-based approaches is that they require a large number of sequential measurements — equal or larger than the number of controllable modes — to determine the focusing wavefront. This limitation can be side-stepped by leveraging the time-reversal symmetry of multiple scattering: if the multiply scattered wave produced by a point source is measured and time-reversed, it will propagate back to focus at the original source position, which allows focusing using a single-shot wavefront measurement. This was first demonstrated for multiple scattering compensation in acoustics by time-reversal mirrors [24] and in optics by nonlinear crystals [60]. In recent years, digital phase-conjugation using computer-controlled SLMs has replaced the analog nonlinear crystal-based approach, as digital phase-conjugation offers simplicity and flexibility not only for coherent scattered light [61], but also using nonlinear [62] and fluorescence [63] signals.

Optical imaging in soft tissues can leverage the fact that acoustic waves essentially do not experience scattering, to produce guide stars on demand. Such ultrasound-mediated guidance can be realized in two ways: either via ultrasonic detection of acoustic signals generated by the photo-acoustic effect, following optical absorption [64], or using localized acousto-optic modulation of light by focused ultrasound [65]. Similarly to all-optical techniques, focusing can be achieved via iterative optimization [66, 67], by computational analysis of a photoacoustically or acousto-optically measured scattering matrix [68, 69] or via phase-conjugation [65]. The major drawback of acousto-optic and photoacoustic guide-stars is that the guide-star dimensions are dictated by the acoustic wavelength — orders of magnitude larger than the optical diffraction limit. Reducing the size of the acousto-optically guided focus can be effectively achieved by iterative phase-conjugation [70], where the phase-conjugation and acousto-optic modulation process is repeated several times, shrinking the size of the focus in each iteration. Mathematically, iterative phase-conjugation is equivalent to raising the reflection matrix to the power of the number of iterations. Repeating the process is therefore equivalent to finding the highest singular value of the scattering matrix. The same result can thus be obtained by injecting the first singular vector of the scattering matrix, as was first realized in acoustics [71], and put to use in all-optical [57] and acousto-optical [72, 69] approaches.
When non-monochromatic light focusing is required, for example, when ultrashort pulses are used for multiphoton excitation scattering may also induce temporal distortions, which will require correction in addition to the spatial distortions. Strikingly, temporal control can be obtained by controlling only

the spatial degrees of freedom, as result of the spatio-temporal coupling of multiple scattering [73].

3.4.3 From focusing to imaging

The ability to form a focus by itself is not enough for imaging. However, it may enable imaging if the focus can be scanned over a sufficiently large FoV, effectively realizing a laser-scanning imaging system. Such scanning is indeed directly possible within the limited FoV of the optical memory-effect [74] (Fig. 4b) (see Box 1). As an alternative to focus scanning, one can exploit the fact that, in most instances in optics, Helmholtz reciprocity allows exchanging the source and the detector without changing the result. As a result, the memory effect also means that all the points within the isoplanatic patch can be corrected simultaneously by placing the SLM in the detection path instead of the illumination path. Thus, if the wavefront correction for a point is known, it is possible to use it to perform wide-field single-shot imaging [35] (Fig.4c).

3.4.4 Computational imaging through complex media

A very promising direction for imaging that does not require physical correction of scattering and can be implemented without a wavefront shaping device, is the use of computational image reconstruction. As suggested by Freund three decades ago [22], memory effect-based imaging can be possible even without knowledge or measurement of the scattering-matrix. The first realization in multiply-scattering media was demonstrated by scanning unknown but correlated speckle patterns over a fluorescence target (Fig.3a) and recording the total fluorescence signal excited by each pattern [75]. The measured fluorescence signal intensity is proportional to the overlap between the speckle pattern and the target object, and its intensity as a function of scanning angle therefore provides the convolution of the object with the unknown speckle pattern. As the spatial autocorrelation of a speckle pattern is a diffraction limited peak [20], the autocorrelation of the scan trace provides the target object autocorrelation, and the object image can be computationally reconstructed via phase-retrieval [76] or bi-spectrum [77] reconstruction techniques adapted from astronomy. Thanks to Helmholtz reciprocity, a similar measurement can be performed in a single shot [51, 78] (Fig.4c), bringing Labeyrie's stellar speckle interferometry [79] from astronomy to complex media.

The FoV limitation of the memory effect can be overcome by stitching multiple measurements, where each measurement images a FoV smaller than the isoplanatic patch size. This was recently demonstrated by decomposition of the reflection matrix to several isoplanatic corrections [80, 25], non-negative matrix factorization of the fluorescence scattering matrix [55] or sequential acousto-optic modulation of small isoplanatic patches [81]. Such advanced computational reconstructions not only allow a wider FoV, but also provide a more stable convergence compared to iterative phase-retrieval.

Computational reconstruction approaches have also been put forward to im-

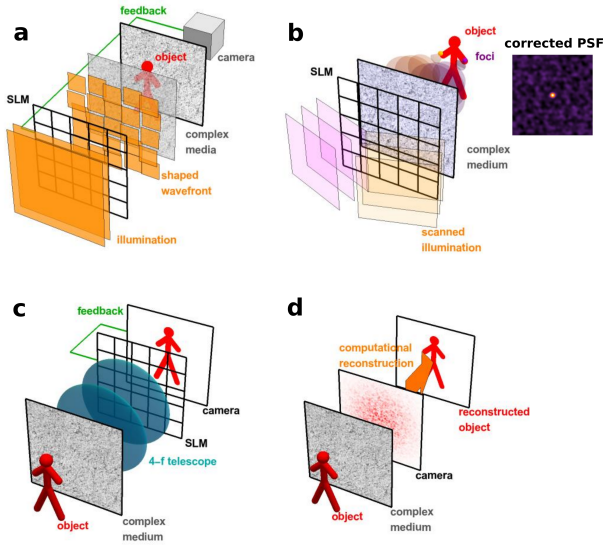

Figure 4: Different approaches for imaging via wavefront-shaping. (a) The illumination wavefront is shaped by a spatial light modulator (SLM) such that its interference after scattering by the complex medium forms a sharp diffraction-limited focus on the target (inset: 'corrected PSF'). The optimal focusing wavefront is found by feedback from a detector or camera, potentially utilizing optical or acoustical modulation techniques, or both. (b) The memory-effect allows simple scanning of the formed focus across all points within the isoplanatic patch by simple tilt of the correction wavefront; (c) similarly, via Helmholtz reciprocity, a single wavefront correction can simultaneously correct all points within the memory-effect field of view for widefield imaging; (d) widefield imaging can be performed computationally from scattered-light measurements, without a physical correction.

prove the resolution of acousto-optic and photo-acoustic tomographic techniques. Random dynamic speckle illumination can improve the imaging fidelity and resolution of photoacoustic and acousto-optic tomography [82, 83, 84], as randomly fluctuating speckle grains allows the adaptation of super-resolution optical fluctuation imaging (SOFI) [85] to ultrasound-mediated imaging. Flow-induced fluctuations were also utilized for super resolved photoacoustics, either via super-resolution optical fluctuation imaging [86] or localization of flowing absorbers [87, 88, 89, 90]. These approaches surpass the acoustic resolution and allow a very wide FoV but generally do not reach the optical diffraction limit.

Deep-learning (DL) neural-network based approaches for imaging using scattered light are still in their infancy, but carry great potential to improve the reconstruction fidelity while alleviating the requirements for exact modelling,

number of measurements, and the accuracy and stability of the optical setup. Similar to scattering matrix-based approaches [29], deep-learning can be applied to solve the inverse problem of recovering the object information from a dataset of scattered-light measurements [91, 92, 93, 94], effectively incorporating learned regularization, better estimation of the scattering-matrix and generalization of speckle correlations. However, because coherent light propagation and speckle patterns are not present in most common imaging problems, the conventional network architectures used in those situations are not optimal for imaging in complex media. To go beyond the performance of non-DL scattering-matrix-based approaches, recent DL works utilized a hybrid model-based or physics-informed network architecture [95], allowing to retrieve not just the object information, but also the parameters of the optical setup [96, 97].

3.5 Imaging through optical fibres

While one would always prefer imaging techniques to be non-invasive, this is not always possible. For imaging at very large depths, absorption ultimately limits information transmission, and minimally-invasive techniques, such as endoscopy, which are based on the insertion of a small diameter probe to bypass scattering and absorption, are used [98]. Fibre-based endoscopic probes are a common solution. However, their diameter is typically larger than the imaged FoV due to the use of lenses or scanners at the distal fibre end or aberrations in graded-index rod-lenses. A lens-less endoscope, based on a small-diameter bare fibre is thus a highly attractive solution.

As the scattering-matrix formalism also describes light propagation through optical fibrer, the same techniques used for focusing and imaging in complex media can be employed to realize lens-less bare-fibre endoscopes. The reason that the scattering matrix of the fibre is required to reconstruct the optical field at the distal end from its measurements at the proximal end is that multi-mode propagation through a fibre — be it a multimode fibre (MMF) or a multicore fibre (MCF) — induces different phase accumulation for the different modes, resulting in a complex speckle pattern, similar to the one produced by multiple scattering, after propagation [99].

An image was first projected through a multimode fibre in the 1960s [100], but measuring the transmission matrix of a fibre only became feasible [101, 102] with the advent of digital holography and wavefront shaping. As in complex media, imaging can be performed computationally [103] or by scanning a wavefront-shaped focus [102, 104]. However, unless the fibre is kept static, for example, fixed inside a stiff needle, its transmission matrix will change upon any bending or even temperature change [105]. Thus, noninvasive in-situ calibration is a requirement for imaging through flexible fibres. Like in complex media, non-invasive focusing and imaging is possible by using a nonlinear guide-star [106], decomposing the reflection matrix [107] or by placing engineered reflecting layers next to the distal fibre tip [108, 109]. Imaging in MMFs can be performed through the knowledge of the entire matrix or by partial knowledge of the transmission matrix exploiting the rotational memory-effect present in cylindrically

symmetric (unperturbed) fibres [110, 111]. Alternatively, if the precise structure and bending of the fibre are known, it is possible to predict the changes in the transmission matrix [105]. Designing fibres with reduced sensitivity to bending is also an ongoing effort [112, 113].
Fibre bundles composed of thousands of individual few-mode fibres (Fig.4c), are especially interesting systems, as the small coupling between cores leads to a propagation that is equivalent to a thin scattering layer (or diffuser). They thus possess the conventional angular memory effect, and it is possible to exploit it in similar fashions as for scattering media [104, 114]. It is worth mentioning that, although single-mode fibrer have only one spatial degree of freedom, imaging information can nonetheless be transmitted in their spectral (or equivalently, temporal) degrees of freedom by placing a spatio-spectral encoder at the fibre distal end [115]. As in scattering media, deep-learning-based approaches have found use in computational imaging through fibres and are under intense study [116, 92].
Figure 5 presents some recent results for diffraction-limited noninvasive imaging through complex media, either via physical correction (Fig.5a-c) or computational reconstruction (Fig.5d-f).

3.6 Discussion

Scattering in complex media makes imaging information difficult to retrieve. Until recently this was practically an intractable problem, but advances in the available technology, computational approaches and our understanding of multiple scattering, have led to a flourish of novel techniques and surprising results. The various approaches have emerged from different communities, and are often useful in different regimes. As a result, the nomenclature, formalism and descriptions may vary considerably from one community to another. This may intimidate newcomers, but as is often the case, the various techniques are more similar than they appear to be on the surface. The scattering matrix formalism provides a unified framework to describe the different approaches, highlighting the similarities and encouraging communication between fields.
The topic of imaging in complex media has evolved rapidly, producing many astonishing results, but with a few exceptions these results have not yet percolated to the imaging community at large. One major reason for this is that many approaches only work well in some very specific circumstances, which those working on real-world applications may find too restrictive. Therefore, a major challenge that needs to be tackled in the near future is how to overcome this gap. This will necessitate technological advancements, including faster and more sensitive detectors, to allow the measurement of the **S**-matrix within the sample decorrelation time, but mostly it will require combining ideas from fields that approach the problem from different directions.
That said, it is unlikely that a universal technique, able to perform imaging in all scattering regimes, will ever appear. What is more likely is that a number of techniques will be developed, each suitable for a specific real-world situation — making a unified framework and ease of communication between fields even

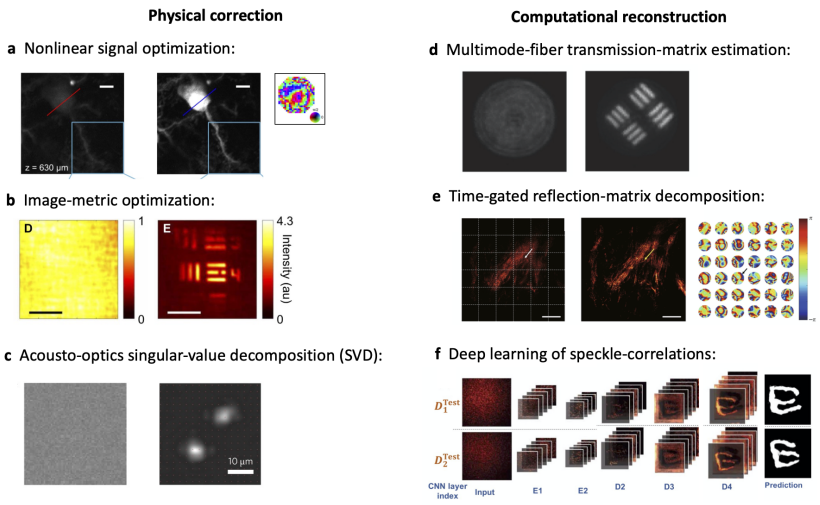

Figure 5: Examples for diffraction-limited images obtained noninvasively through complex media with various approaches: **(a-c)** Physical correction of scattering using wavefront shaping, where the correction is found by: **(a)** nonlinear signal optimization [50] , **(b)** image-metric optimization [54], and **(c)** singular-value decomposition (SVD) of acousto-optically tagged speckle patterns [72]. **(d-f)** Computational reconstruction via: **(d)** estimation of a multimode-fiber (MMF) transmission matrix from physical fibre parameters [105], **(e)** decomposition of the time-gated reflection-matrix [117], and **(f)** deep learning of speckle-correlations [93]. Left panels display the conventionally captured, uncorrected images. Right panels in (a-d,f) and middle panel in (e) display the corrected images. Inset in (a) and right panel in (e) display the applied wavefront corrections.

more important.

Acknowledgments

J.B. acknowledges funding from the Engineering and Physical Sciences Research Council (EPSRC) EP/T00097X/1. O.K. acknowledges funding from the European Research Council under the European Union's Horizon 2020 Research and Innovation Program Grant n° 101002406 and the Israel Science Foundation (1361/18).

References

[1] P. Sheng, *Introduction to Wave Scattering, Localization and Mesoscopic Phenomena*. Springer, 2010.

[2] E. Akkermans and G. Montambaux, *Mesoscopic Physics of Electrons and Photons*. Cambridge University Press, 2007.

[3] R. Carminati and J. C. Schotland, *Principles of scattering and transport of light*. Cambridge University Press, 2021.

[4] D. S. Richardson and J. W. Lichtman, "Clarifying tissue clearing," *Cell*, vol. 162, p. 246, 2015.

[5] A. J. Chen H, Rogalski MM, "Advances in functional x-ray imaging techniques and contrast agents," *Phys Chem Chem Phys.*, vol. 14, p. 13469, 2012.

[6] T. L. Szabo, *Diagnostic Ultrasound Imaging: Inside Out*. Elsevier, 2014.

[7] A. McCarthy, R. J. Collins, N. J. Krichel, V. Fernández, A. M. Wallace, and G. S. Buller, "Long-range time-of-flight scanning sensor based on high-speed time-correlated single-photon counting," *Appl. Opt.*, vol. 48, p. 6241, 2009.

[8] D. Huang, E. A. Swanson, C. P. Lin, J. S. Schuman, W. G. Stinson, W. Chang, M. R. Hee, T. Flotte, K. Gregory, C. A. Puliafito, and J. G. Fujimoto, "Optical coherence tomography," *Science*, vol. 254, p. 1178, 1991.

[9] J. Pawley, ed., *Handbook Of Biological Confocal Microscopy*. Springer, 2006.

[10] W. R. Zipfel, R. M. Williams, and W. W. Webb, "Nonlinear magic: multiphoton microscopy in the biosciences," *Nature biotechnology*, vol. 21, no. 11, pp. 1369–1377, 2003.

[11] P. Theer and W. Denk, "On the fundamental imaging-depth limit in two-photon microscopy," *J. Opt. Soc. Am. A*, vol. 23, p. 3139, 2006.

[12] N. G. Horton, K. Wang, D. Kobat, C. G. Clark, F. W. Wise, C. B. Schaffer, and C. Xu, "In vivo three-photon microscopy of subcortical structures within an intact mouse brain," *Nature photonics*, vol. 7, no. 3, pp. 205–209, 2013.

[13] A. Badon, D. Li, G. Lerosey, A. C. Boccara, M. Fink, and A. Aubry, "Smart optical coherence tomography for ultra-deep imaging through highly scattering media," *Science Advances*, vol. 2, p. e1600370, 2016.

[14] S. Yoon, M. Kim, M. Jang, Y. Choi, W. Choi, S. Kang, and W. Choi, "Deep optical imaging within complex scattering media," *Nature Reviews Physics*, vol. 2, p. 141, 2020.

[15] Cao, Rotter, and Mosk *in this issue*, 2022.

[16] W. Choi, A. P. Mosk, Q.-H. Park, and W. Choi, "Transmission eigenchannels in a disordered medium," *Phys. Rev. B*, vol. 83, p. 134207, 2011.

[17] H. Yılmaz, C. W. Hsu, A. Yamilov, and H. Cao, "Transverse localization of transmission eigenchannels," *Nature Photonics*, vol. 13, p. 352, 2019.

[18] J. Carpenter, B. J. Eggleton, and J. Schröder, "Observation of eisenbud–wigner–smith states as principal modes in multimode fibre," *Nature Photonics*, vol. 9, p. 751, 2015.

[19] J. W. Goodman, *Introduction to Fourier optics*. Roberts & Company, 2005.

[20] J. W. Goodman, *Speckle Phenomena in Optics: Theory and Applications*. SPIE, 2020.

[21] S. Feng, C. Kane, P. A. Lee, and A. D. Stone, "Correlations and fluctuations of coherent wave transmission through disordered media," *Phys. Rev. Lett.*, vol. 61, pp. 834–837, Aug 1988.

[22] I. Freund, "Looking through walls and around corners," *Physica A*, vol. 168, pp. 49–65, 1990.

[23] R. Davies and M. Kasper, "Adaptive optics for astronomy," *Annual Review of Astronomy and Astrophysics*, vol. 50, p. 305, 2012.

[24] M. Fink, D. Cassereau, A. Derode, C. Prada, P. Roux, M. Tanter, J.-L. Thomas, and F. Wu, "Time-reversed acoustics," *Reports on progress in Physics*, vol. 63, no. 12, p. 1933, 2000.

[25] A. Badon, V. Barolle, K. Irsch, A. Boccara, M. Fink, and A. Aubry, "Distortion matrix concept for deep optical imaging in scattering media," *Science Advances*, vol. 6, no. 30, p. eaay7170, 2020.

[26] T. Blondel, J. Chaput, A. Derode, M. Campillo, and A. Aubry, "Matrix approach of seismic imaging: Application to the erebus volcano, antarctica," *JGR Solid Earth*, vol. 123, p. 10936, 2018.

[27] S. Arridge, "Methods in diffuse optical imaging," *Phil. Trans. R. Soc. A*, vol. 369, p. 4558, 2011.

[28] A. Gibson, J. Hebden, and S. Arridge, "Recent advances in diffuse optical imaging," *Phys. Med. Biol.*, vol. 50, no. 4, p. R1, 2005.

[29] S. Popoff, G. Lerosey, M. Fink, A. C. Boccara, and S. Gigan, "Image transmission through an opaque material," *Nat. Commun.*, vol. 1, p. 81, 2010.

[30] A. Liutkus, D. Martina, S. Popoff, G. Chardon, O. Katz, G. Lerosey, S. Gigan, D. L, and I. Carron *Scientific Reports*, vol. 4, p. 5552, 2014.

[31] S. M. Popoff, G. Lerosey, R. Carminati, M. Fink, A. C. Boccara, and S. Gigan, "Measuring the transmission matrix in optics: An approach to the study and control of light propagation in disordered media," *Phys. Rev. Lett.*, vol. 104, p. 100601, 2010.

[32] E. G. van Putten, D. Akbulut, J. Bertolotti, W. L. Vos, A. Lagendijk, and A. P. Mosk, "Scattering lens resolves sub-100 nm structures with visible light," *Phys. Rev. Lett.*, vol. 106, p. 193905, May 2011.

[33] Y. Choi, T. Yang, C. Fang-Yen, P. Kang, K. Lee, R. Dasari, M. Feld, and W. Choi, "Overcoming the diffraction limit using multiple light scattering in a highly disordered medium," *Phys. Rev. Lett.*, vol. 107, p. 023902, 2011.

[34] B. Judkewitz, R. Horstmeyer, I. Vellekoop, P. I.N., and C. Yang, "Translation correlations in anisotropically scattering media," *Nature Physics*, vol. 11, p. 684, 2015.

[35] O. Katz, E. Small, and Y. Silberberg, "Looking around corners and through thin turbid layers in real time with scattered incoherent light," *Nature Photon*, vol. 6, p. 549, 2012.

[36] D. Faccio, A. Velten, and G. Wetzstein, "Non-line-of-sight imaging," *Nature Reviews Physics*, vol. 2, no. 6, pp. 318–327, 2020.

[37] S. Schott, J. Bertolotti, J.-F. Léger, L. Bourdieu, and S. Gigan, "Characterization of the angular memory effect of scattered light in biological tissues," *Opt. Express*, vol. 23, p. 13505, 2015.

[38] M. Kadobianskyi, I. Papadopoulos, T. Chaigne, R. Horstmeyer, and B. Judkewitz, "Scattering correlations of time-gated light," *Optica*, vol. 5, p. 389, 2018.

[39] G. Osnabrugge, R. Horstmeyer, I. Papadopoulos, B. Judkewitz, and I. Vellekoop, "Generalized optical memory effect," *Optica*, vol. 4, p. 886, 2017.

[40] N. Ji, "Adaptive optical fluorescence microscopy," *Nat Methods*, vol. 14, p. 374, 2017.

[41] T. Wu, P. Berto, and M. Guillon, "Reference-less complex wavefields characterization with a high-resolution wavefront sensor," *Applied Physics Letters*, vol. 118, no. 25, p. 251102, 2021.

[42] I. M. Vellekoop and A. P. Mosk, "Focusing coherent light through opaque strongly scattering media," *Opt. Lett.*, vol. 32, pp. 2309–2311, 2007.

[43] I. M. Vellekoop and A. P. Mosk, "Universal optimal transmission of light through disordered materials," *Phys. Rev. Lett.*, vol. 101, no. 12, 2008.

[44] A. P. Mosk, A. Lagendijk, G. Lerosey, and M. Fink, "Controlling waves in space and time for imaging and focusing in complex media," *Nature Photonics*, vol. 6, p. 283, 2012.

[45] I. Vellekoop, "Feedback-based wavefront shaping," *Opt. Express*, vol. 23, p. 12189, 2015.

[46] H. Yilmaz, E. van Putten, J. Bertolotti, A. Lagendijk, W. Vos, and A. Mosk, "Speckle correlation resolution enhancement of wide-field fluorescence imaging," *Optica*, vol. 2, p. 424, 2015.

[47] G. Lerosey, J. de Rosny, A. Tourin, and M. Fink, "Focusing beyond the diffraction limit with far-field time reversal," *Science*, vol. 315, p. 1120, 2007.

[48] J. Tang, R. Germain, and M. Cui, "Superpenetration optical microscopy by iterative multiphoton adaptive compensation technique," *PNAS*, vol. 109, p. 8434, 2012.

[49] I. Papadopoulos, J. Jouhanneau, N. Takahashi, D. Kaplan, M. Larkum, J. Poulet, and B. Judkewitz, "Dynamic conjugate f-sharp microscopy," *Light Sci Appl*, vol. 9, p. 110, 2020.

[50] C. Berlage, M. L. S. Tantirigama, M. Babot, D. D. Battista, C. Whitmire, I. N. Papadopoulos, J. F. A. Poulet, M. Larkum, and B. Judkewitz, "Deep tissue scattering compensation with three-photon f-sharp," *Optica*, vol. 8, pp. 1613–1619, Dec 2021.

[51] O. Katz, P. Heidmann, M. Fink, and S. Gigan, "Non-invasive single-shot imaging through scattering layers and around corners via speckle correlations," *Nature Phot*, vol. 8, p. 784, 2014.

[52] A. Boniface, B. Blochet, J. Dong, and S. Gigan, "Noninvasive light focusing in scattering media using speckle variance optimization," *Optica*, vol. 6, p. 1381, 2019.

[53] A. Daniel, D. Oron, and Y. Silberberg, "Light focusing through scattering media via linear fluorescence variance maximization, and its application for fluorescence imaging," *Opt. Express*, vol. 27, p. 21778, 2019.

[54] T. Yeminy and O. Katz, "Guidestar-free image-guided wavefront shaping," *Science Advances*, vol. 7, p. eabf5364, 2021.

[55] A. Boniface, J. Dong, and S. Gigan, "Non-invasive focusing and imaging in scattering media with a fluorescence-based transmission matrix," *Nat Commun*, vol. 11, p. 6154, 2020.

[56] G. Stern and O. Katz, "Noninvasive focusing through scattering layers using speckle correlations," *Opt. Lett.*, vol. 44, p. 143, 2019.

[57] S. M. Popoff, A. Aubry, G. Lerosey, M. Fink, A. C. Boccara, and S. Gigan, "Exploiting the time-reversal operator for adaptive optics, selective focusing, and scattering pattern analysis," *Phys. Rev. Lett.*, vol. 107, p. 263901, Dec 2011.

[58] S. Kang, S. Jeong, W. Choi, H. Ko, T. Yang, J. Joo, J.-S. Lee, Y.-S. Lim, Q.-H. Park, and W. Choi, "Imaging deep within a scattering medium using collective accumulation of single-scattered waves," *Nature Photon*, vol. 9, p. 253, 2015.

[59] A. Thendiyammal, G. Osnabrugge, T. Knop, and I. M. Vellekoop, "Model-based wavefront shaping microscopy," *Optics letters*, vol. 45, no. 18, pp. 5101–5104, 2020.

[60] Z. Yaqoob, D. Psaltis, M. Feld, and C. Yang, "Optical phase conjugation for turbidity suppression in biological samples," *Nature Photon*, vol. 2, p. 110, 2008.

[61] M. Cui and C. Yang, "Implementation of a digital optical phase conjugation system and its application to study the robustness of turbidity suppression by phase conjugation," *Optics Expr*, vol. 18, p. 3444, 2010.

[62] C. Hsieh, Y. Pu, R. Grange, G. Laporte, and D. Psaltis, "Imaging through turbid layers by scanning the phase conjugated second harmonic radiation from a nanoparticle," *Optics Expr*, vol. 18, p. 20723, 2010.

[63] I. Vellekoop, M. Cui, and C. Yang, "Digital optical phase conjugation of fluorescence in turbid tissue," *Appl Phys Lett*, vol. 101, p. 081108, 2012.

[64] M. Xu and L. V. Wang, "Photoacoustic imaging in biomedicine," *Review of Scientific Instruments*, vol. 77, p. 041101, Apr. 2006.

[65] X. Xu, H. Liu, and L. V. Wang, "Time-reversed ultrasonically encoded optical focusing into scattering media," *Nature photonics*, vol. 5, no. 3, pp. 154–157, 2011.

[66] F. Kong, R. H. Silverman, L. Liu, P. V. Chitnis, K. K. Lee, and Y.-C. Chen, "Photoacoustic-guided convergence of light through optically diffusive media," *Optics letters*, vol. 36, no. 11, pp. 2053–2055, 2011.

[67] P. Lai, L. Wang, J. W. Tay, and L. V. Wang, "Photoacoustically guided wavefront shaping for enhanced optical focusing in scattering media," *Nature photonics*, vol. 9, no. 2, pp. 126–132, 2015.

[68] T. Chaigne, O. Katz, A. C. Boccara, M. Fink, E. Bossy, and S. Gigan, "Controlling light in scattering media non-invasively using the photoacoustic transmission matrix," *Nature Photonics*, vol. 8, no. 1, pp. 58–64, 2014.

[69] O. Katz, F. Ramaz, S. Gigan, and M. Fink, "Controlling light in complex media beyond the acoustic diffraction-limit using the acousto-optic transmission matrix," *Nature Communications*, vol. 10, Feb. 2019.

[70] K. Si, R. Fiolka, and M. Cui, "Breaking the spatial resolution barrier via iterative sound-light interaction in deep tissue microscopy," *Scientific Reports*, vol. 2, Oct. 2012.

[71] C. Prada, S. Manneville, D. Spoliansky, and M. Fink, "Decomposition of the time reversal operator: Detection and selective focusing on two scatterers," *The Journal of the Acoustical Society of America*, vol. 99, no. 4, pp. 2067–2076, 1996.

[72] B. Judkewitz, Y. M. Wang, R. Horstmeyer, A. Mathy, and C. Yang, "Speckle-scale focusing in the diffusive regime with time reversal of variance-encoded light (TROVE)," *Nature Photonics*, vol. 7, pp. 300–305, Mar. 2013.

[73] J. Aulbach, B. Gjonaj, P. Johnson, A. Mosk, and A. Lagendijk, "Control of light transmission through opaque scattering media in space and time," *Phys. Rev. Lett.*, vol. 106, p. 103901, 2011.

[74] I. Vellekoop and C. Aegerter, "Scattered light fluorescence microscopy: imaging through turbid layers," *Opt. Lett.*, vol. 35, p. 1245, 2010.

[75] J. Bertolotti, E. van Putten, C. Blum, A. Lagendijk, W. Vos, and A. Mosk, "Non-invasive imaging through opaque scattering layers," *Nature*, vol. 491, p. 232, 2012.

[76] J. R. Fienup, "Reconstruction of an object from the modulus of its fourier transform," *Opt. Lett.*, vol. 3, no. 1, p. 27, 1978.

[77] T. Wu, O. Katz, X. Shao, and S. Gigan, "Single-shot diffraction-limited imaging through scattering layers via bispectrum analysis," *Opt. Lett.*, vol. 41, p. 5003, 2016.

[78] M. Hofer, C. Soeller, S. Brasselet, and J. Bertolotti, "Wide field fluorescence epi-microscopy behind a scattering medium enabled by speckle correlations," *Opt. Expr.*, vol. 26, p. 9866, 2018.

[79] A. Labeyrie *Astron. Astrophys.*, vol. 6, p. 85, 1970.

[80] S. Kang, P. Kang, S. Jeong, Y. Kwon, T. Yang, J. Hong, M. Kim, K.-D. Song, J. Park, J. Lee, M. Kim, K. Kim, and W. Choi, "High-resolution adaptive optical imaging within thick scattering media using closed-loop accumulation of single scattering," *Nature comm*, vol. 8, p. 2157, 2017.

[81] M. Rosenfeld, G. Weinberg, D. Doktofsky, Y. Li, L. Tian, and O. Katz, "Acousto-optic ptychography," *Optica*, vol. 8, p. 936, 2021.

[82] J. Gateau, T. Chaigne, O. Katz, S. Gigan, and E. Bossy, "Improving visibility in photoacoustic imaging using dynamic speckle illumination," *Opt. Lett.*, vol. 38, pp. 5188–5191, Dec 2013.

[83] T. Chaigne, J. Gateau, M. Allain, O. Katz, S. Gigan, A. Sentenac, and E. Bossy, "Super-resolution photoacoustic fluctuation imaging with multiple speckle illumination," *Optica*, vol. 3, p. 54, 2016.

[84] D. Doktofsky, M. Rosenfeld, and O. Katz, "Acousto optic imaging beyond the acoustic diffraction limit using speckle decorrelation," *Communications Physics*, vol. 3, no. 1, pp. 1–8, 2020.

[85] T. Dertinger, R. Colyer, G. Iyer, S. Weiss, and J. Enderlein, "Fast, background-free, 3d super-resolution optical fluctuation imaging (sofi)," *PNAS*, vol. 106, p. 22287, 2009.

[86] T. Chaigne, B. Arnal, S. Vilov, E. Bossy, and O. Katz, "Super-resolution photoacoustic imaging via flow-induced absorption fluctuations," *Optica*, vol. 4, no. 11, pp. 1397–1404, 2017.

[87] X. L. Dean-Ben and D. Razansky, "Localization optoacoustic tomography," *Light, science & applications*, vol. 7, p. 18004, 2018.

[88] J. Kim, J. Y. Kim, S. Jeon, J. W. Baik, S. H. Cho, and C. Kim, "Super-resolution localization photoacoustic microscopy using intrinsic red blood cells as contrast absorbers," *Light: Science & Applications*, vol. 8, no. 1, pp. 1–11, 2019.

[89] P. Zhang, L. Li, L. Lin, J. Shi, and L. V. Wang, "In vivo superresolution photoacoustic computed tomography by localization of single dyed droplets," *Light: Science & Applications*, vol. 8, no. 1, pp. 1–9, 2019.

[90] S. Vilov, B. Arnal, and E. Bossy, "Overcoming the acoustic diffraction limit in photoacoustic imaging by the localization of flowing absorbers," *Optics letters*, vol. 42, no. 21, pp. 4379–4382, 2017.

[91] S. Li, M. Deng, J. Lee, A. Sinha, and G. Barbastathis, "Imaging through glass diffusers using densely connected convolutional networks," *Optica*, vol. 5, p. 803, 2018.

[92] P. Caramazza, O. Moran, R. Murray-Smith, and D. Faccio, "Transmission of natural scene images through a multimode fibre," *Nature communications*, vol. 10, no. 1, pp. 1–6, 2019.

[93] Y. Li, Y. Xue, and L. Tian, "Deep speckle correlation: a deep learning approach toward scalable imaging through scattering media," *Optica*, vol. 5, p. 1181, 2018.

[94] Y. Li, S. Cheng, Y. Xue, and L. Tian, "Displacement-agnostic coherent imaging through scatter with an interpretable deep neural network," *Opt. Express*, vol. 29, p. 2244, 2021.

[95] K. Monakhova, J. Yurtsever, G. Kuo, N. Antipa, K. Yanny, and L. Waller, "Learned reconstructions for practical mask-based lensless imaging," *Optics express*, vol. 27, no. 20, pp. 28075–28090, 2019.

[96] M. W. Matthès, Y. Bromberg, J. de Rosny, and S. M. Popoff, "Learning and avoiding disorder in multimode fibers," *Physical Review X*, vol. 11, no. 2, p. 021060, 2021.

[97] Gigan *in this issue*, 2022.

[98] M. Gu, H. Bao, and H. Kang, "Fibre-optical microendoscopy," *Journal od microscopy*, vol. 254, p. 13, 2014.

[99] K. Okamoto, *Fundamentals of Optical Waveguides*. Elsevier, 2005.

[100] E. Spitz and A. Werts, "Transmission des images à travers une fibre optique," *COMPTES RENDUS HEBDOMADAIRES DES SEANCES DE L'ACADEMIE DES SCIENCES ERIE B*, vol. 264, p. 1015, 1967.

[101] R. Di Leonardo and S. Bianchi, "Hologram transmission through multimode optical fibers," *Optics Express*, vol. 19, p. 24, 2010.

[102] T. Čižmár and K. Dholakia, "Exploiting multimode waveguides for pure fibre-based imaging," *Nature Communications*, vol. 3, 2012.

[103] Y. Choi, C. Yoon, M. Kim, T. D. Yang, C. Fang-Yen, R. R. Dasari, K. J. Lee, and W. Choi, "Scanner-free and wide-field endoscopic imaging by using a single multimode optical fiber," *Phys. Rev. Lett.*, vol. 109, p. 203901, 2012.

[104] E. R. Andresen, G. Bouwmans, S. Monneret, and H. Rigneault, "Toward endoscopes with no distal optics: video-rate scanning microscopy through a fiber bundle," *Opt. Lett.*, vol. 38, pp. 609–611, Mar 2013.

[105] M. Plöschner, T. Tyc, and T. Čižmár, "Seeing through chaos in multimode fibres," *Nature Photonics*, vol. 9, pp. 529–535, July 2015.

[106] U. Weiss and O. Katz, "Two-photon lensless micro-endoscopy with in-situ wavefront correction," *Opt. Express*, vol. 26, pp. 28808–28817, Oct 2018.

[107] W. Choi, M. Kang, J. H. Hong, O. Katz, Y. Choi, and W. Choi, "Fourier holographic endoscopy for label-free imaging through a narrow and curved passage," *arXiv preprint arXiv:2010.11776*, 2020.

[108] G. S. D. Gordon, M. Gataric, A. G. C. P. Ramos, R. Mouthaan, C. Williams, J. Yoon, T. D. Wilkinson, and S. E. Bohndiek, "Characterizing optical fiber transmission matrices using metasurface reflector stacks for lensless imaging without distal access," *Phys. Rev. X*, vol. 9, p. 041050, Dec 2019.

[109] R. Kuschmierz, E. Scharf, N. Koukourakis, and J. W. Czarske, "Self-calibration of lensless holographic endoscope using programmable guide stars," *Opt. Lett.*, vol. 43, pp. 2997–3000, Jun 2018.

[110] L. V. Amitonova, A. P. Mosk, and P. W. H. Pinkse, "Rotational memory effect of a multimode fiber," *Opt. Express*, vol. 23, pp. 20569–20575, Aug 2015.

[111] S. Li, S. A. R. Horsley, T. Tyc, T. Čižmár, and D. B. Phillips, "Memory effect assisted imaging through multimode optical fibres," *Nature Communications*, vol. 12, June 2021.

[112] D. E. Boonzajer Flaes, J. Stopka, S. Turtaev, J. F. de Boer, T. Tyc, and T. Čižmár, "Robustness of light-transport processes to bending deformations in graded-index multimode waveguides," *Phys. Rev. Lett.*, vol. 120, p. 233901, Jun 2018.

[113] V. Tsvirkun, S. Sivankutty, K. Baudelle, R. Habert, G. Bouwmans, O. Vanvincq, E. R. Andresen, and H. Rigneault, "Flexible lensless endoscope with a conformationally invariant multi-core fiber," *Optica*, vol. 6, no. 9, pp. 1185–1189, 2019.

[114] N. Stasio, C. Moser, and D. Psaltis, "Calibration-free imaging through a multicore fiber using speckle scanning microscopy," *Opt. Lett.*, vol. 41, pp. 3078–3081, Jul 2016.

[115] R. Barankov and J. Mertz, "High-throughput imaging of self-luminous objects through a single optical fibre," *Nature Communications*, vol. 5, Nov. 2014.

[116] B. Rahmani, D. Loterie, G. Konstantinou, D. Psaltis, and C. Moser, "Multimode optical fiber transmission with a deep learning network," *Light: Science & Applications*, vol. 7, Oct. 2018.

[117] M. Kim, Y. Jo, J. H. Hong, S. Kim, S. Yoon, K.-D. Song, S. Kang, B. Lee, G. H. Kim, H.-C. Park, *et al.*, "Label-free neuroimaging in vivo using synchronous angular scanning microscopy with single-scattering accumulation algorithm," *Nature communications*, vol. 10, no. 1, pp. 1–9, 2019.